NIH Public Access
Author Manuscript
*Neuron*. Author manuscript; available in PMC 2015 October 22.

Published in final edited form as:
*Neuron*. 2014 October 22; 84(2): 340–346. doi:10.1016/j.neuron.2014.08.046.

# Presynaptic HCN channels regulate vesicular glutamate transport

**Hai Huang**[1,2] and **Laurence O. Trussell**[1]

[1]Oregon Hearing Research Center & Vollum Institute, Oregon Health and Science University, 3181 SW Sam Jackson Park Road, L335A, Portland, Oregon 97239 USA

[2]Department of Cell and Molecular Biology, Tulane University, 2000 Percival Stern Hall, 6400 Freret Street, New Orleans, LA 70118 USA

## SUMMARY

The amount of neurotransmitter stored in synaptic vesicles determines postsynaptic quantal size and thus the strength of synaptic transmission. However, little is known about regulation of vesicular neurotransmitter uptake. In recordings from the calyx of Held, a giant mammalian glutamatergic synapse, we found that changes in presynaptic $Na^+$ concentration above and below a resting value of 13 mM regulated vesicular glutamate uptake, consistent with activation of a vesicular monovalent cation $Na^+(K^+)/H^+$ exchanger. $Na^+$ flux through presynaptic plasma membrane hyperpolarization-activated cyclic nucleotide-gated (HCN) channels enhanced presynaptic $Na^+$ concentration and thus controlled postsynaptic quantal size. Our results indicate that a plasma membrane ion channel controls synaptic strength by modulating vesicular neurotransmitter uptake through a $Na^+$-dependent process.

### Keywords

vesicular glutamate uptake; HCN channel; quantal size; calyx of Held; axon terminals

## INTRODUCTION

Synaptic vesicles express transporters that drive neurotransmitter accumulation by exploiting the energy stored in a proton ($H^+$) electrochemical gradient ($\Delta\mu_{H+}$) produced by the vacuolar $H^+$-ATPase ($H^+$ pump). The $\Delta\mu_{H+}$ reflects both electrical potential ($\Delta\Psi$) and chemical pH gradients ($\Delta$pH); transporters for different neurotransmitters depend to

© 2014 Elsevier Inc. All rights reserved

*Address correspondence to: Hai Huang, Department of Cell and Molecular Biology, Tulane University, 2000 Percival Stern Hall, 6400 Freret St, New Orleans, LA 70118 USA, Tel: 504-862-3164, Fax: 504-865-6785, hhuang5@tulane.edu.

Author Contributions:
H.H. conducted and analyzed all experiments. H.H. and L.O.T. designed experiments and wrote the manuscript.

**Publisher's Disclaimer:** This is a PDF file of an unedited manuscript that has been accepted for publication. As a service to our customers we are providing this early version of the manuscript. The manuscript will undergo copyediting, typesetting, and review of the resulting proof before it is published in its final citable form. Please note that during the production process errors may be discovered which could affect the content, and all legal disclaimers that apply to the journal pertain.

Competing Financial Interests:
The authors declare no competing financial interests.

NIH-PA Author Manuscript
NIH-PA Author Manuscript
NIH-PA Author Manuscript

NIH-PA Author Manuscript

NIH-PA Author Manuscript

NIH-PA Author Manuscript

differing extents on ΔΨ and ΔpH due to the charge on the substrate and the stoichiometry of coupling to $H^+$ (Hnasko and Edwards, 2012). Previous studies have suggested that glutamate uptake into synaptic vesicles by the vesicular glutamate transporter (VGLUT) is dependent mostly on ΔΨ rather than ΔpH (Maycox et al., 1988; Tabb et al., 1992). However, glutamate entry acidifies synaptic vesicles and accumulates protons, which reduces the $H^+$ pump's capacity to create the ΔΨ required for VGLUT function, therefore stalling the upload of glutamate. Recently, a study showed that synaptic vesicles express a $K^+(Na^+)/H^+$ monovalent cation exchanger activity that converts ΔpH into ΔΨ and promotes synaptic vesicle filling with glutamate (Goh et al., 2011). Manipulating presynaptic $K^+$ influenced miniature excitatory postsynaptic current (mEPSC) amplitude or quantal size even when the glutamate supply is unchanged, indicating that synaptic vesicle $K^+/H^+$ exchange regulates glutamate release and synaptic transmission (Goh et al., 2011). Although intracellular $[K^+]$ is relatively stable, the $Na^+$ concentration is dynamically regulated during activity of plasma membrane ion channels, raising the possibility that $[Na^+]$ may have a regulatory influence on VGLUT activity. Using whole-cell electrophysiology and imaging, we found that changes in presynaptic $Na^+$ indeed affect the quantal size. Presynaptic hyperpolarization-activated cyclic nucleotide-gated (HCN) chancels, which flux both $Na^+$ and $K^+$, controlled intracellular resting $Na^+$ concentration. Activation of these presynaptic channels by voltage or cAMP increased intracellular $Na^+$ concentration, and increased quantal size.

## RESULTS

### Presynaptic intracellular $Na^+$ regulates quantal size

Paired pre- and postsynaptic recordings were made at the calyx of Held, a giant glutamatergic nerve terminal in the medial nucleus of the trapezoid body (MNTB), to examine whether presynaptic $[Na^+]$ influences postsynaptic quantal current. Using whole-cell patch clamp recordings, we dialyzed the cytosolic contents of presynaptic calyces of Held and simultaneously measured the AMPA receptor-mediated glutamatergic postsynaptic response from MNTB principal neurons. Given that glutamate receptors at this synapse are not saturated by a single quantum of transmitter (Hori and Takahashi, 2012; Ishikawa et al., 2002), we were able to detect changes in mEPSC amplitude as a result of changes in vesicular glutamate filling (Goh et al., 2011). The calyces were recorded with pipette solutions containing 0 mM, 10 mM, or 40 mM $Na^+$ and miniature EPSCs (mEPSCs) were recorded from the postsynaptic MNTB neuron (Fig. 1). Immediately after presynaptic break-in to whole-cell mode, we observed no difference in mEPSC amplitude with different $Na^+$ concentrations ($P = 0.92$, ANOVA test). With 10 mM $Na^+$ solution presynaptically, the mEPSC remained stable over 30 min of recording (102 ± 6%; $P = 0.63$, $n = 4$; Fig. 1A). When the terminal was dialyzed with 40 mM $Na^+$ the mEPSC amplitude gradually increased by 22 ± 7% ($P = 0.007$, $n = 5$; Fig. 1B), while upon dialysis with $Na^+$-free solution, the mEPSC amplitude gradually declined by 20 ± 5% ($P = 0.007$, $n = 5$; Fig. 1C). Normalized to the values observed immediately after break-in, mEPSC size was clearly lower in $Na^+$-free than 10 mM $Na^+$ ($P = 0.001$), while bigger in 40 mM $Na^+$ than in 10 mM $Na^+$ ($P = 0.003$, unpaired t-test; Fig. 1G), and the cumulative frequency distribution of mEPSC amplitudes shifted to the left with dialysis in 0 mM $Na^+$, shifted to the right with 40 mM $Na^+$, and was not changed with 10 mM $Na^+$ (Fig. 1D-F). Since the change in $Na^+$ is restricted to the nerve

NIH-PA Author Manuscript

NIH-PA Author Manuscript

NIH-PA Author Manuscript

terminal and does not affect the postsynaptic neuron, these data suggest that the changes in quantal size reflected alteration in vesicular glutamate uptake. To assess if the $Na^+$ effect on quantal size is dependent on $K^+(Na^+)/H^+$ monovalent cation exchanger activity (Goh et al., 2011), we added the $Na^+/H^+$ exchanger inhibitor EIPA (100 μM) to the presynaptic pipette. Dialysis with 40 mM $Na^+$ containing EIPA reduced mEPSC amplitude by 17 ± 3% ($P$ = 0.002, $n$ = 4; Fig. 1G), supporting the involvement of an vesicular $Na^+/H^+$ exchanger activity. It should be noted that the presynaptic $K^+$ was kept constant (92 mM) in all conditions, showing that dynamic change of $Na^+$ alone can affect the glutamate uptake. Moreover, the magnitude of these changes is comparable to that seen for the virtual elimination of presynaptic $K^+$ (Goh et al., 2011) highlighting a greater sensitivity to changes in $Na^+$ than $K^+$.

## Presynaptic HCN channels control resting $Na^+$ concentration

Since presynaptic $[Na^+]$ affects glutamate uptake, we asked whether intracellular $[Na^+]$ can be manipulated by plasma membrane ion channels. The focus was on the $Na^+$-permeable HCN channel because this channel is active at the resting potential and indeed constitutes a major component of the resting membrane conductance (Huang and Trussell, 2011). Thus, it would be expected that these channels could supply a continuous inward flux of $Na^+$. Whole-cell recordings from calyces were made and the $Na^+$ change was assayed using two-photon laser scanning microscopy. Calyces were loaded via patch pipettes with the volume marker Alexa 594 (20 μM) and the $Na^+$ indicator SBFI (1 mM). Cell morphology was assessed by visualizing Alexa 594 or SBFI after the two dyes filled the terminal (Fig. 2A). Line-scans or frame-scans were made on calyces, and $Na^+$ changes were measured by change in fluorescence. Standard calibration methods were used to measure the absolute $[Na^+]$ (see Experimental Procedures), which revealed an apparent $K_d$ ($K_{app}$) of 22 mM and $(G/R)_{max}$ of 0.78 for SBFI (Supplemental Fig. S1). The presynaptic $[Na^+]$ at the resting state was 12.7 ± 2.4 mM (n = 6). In the presence of tetrodotoxin (TTX) to block voltage-gated $Na^+$ channels, a voltage step from −60 mV to −100 mV evoked an inward current (Fig. 2B). Meanwhile, SBFI fluorescence was decreased by 12.2 ± 1.2% ($P$ < 0.0001, n = 10) upon the activation of HCN channel, indicating an increase of resting $[Na^+]$ of 4.9 ± 0.5 mM (n = 10). Both the inward current and $Na^+$ signal were blocked by HCN channel blocker CsCl (2 mM), confirming that the $Na^+$ increase was mediated by activation of HCN channels (Fig. 2B).

Consistent with previous findings that hyperpolarization-activated HCN channels begin to activate at a voltage more depolarized than the resting membrane potential and therefore contribute to the resting conductance (Cuttle et al., 2001; Huang and Trussell, 2011), we found that blocking HCN channels with CsCl (1-2 mM) hyperpolarized the calyx by 3 mV (Supplemental Fig. S2; from −73.2 ± 1.6 mM to −76.1 ± 1.8 mV; $P$ = 0.01, n = 4). Since HCN channels are $Na^+$-permeable, it is likely that HCN channels could affect the resting $[Na^+]$. After whole-cell dialysis with SBFI and Alexa 594 dyes, the recording pipettes were subsequently detached from calyces and the $Na^+$ signals were measured. We found that blocking HCN channels with CsCl reversibly reduced the resting $[Na^+]$ by 4.5 ± 0.3 mM ($P$ < 0.001, n = 6; Fig. 2C). The hyperpolarization caused by blocking HCN channels (Supplemental Fig. S2) would be expected to deactivate persistent $Na^+$ channels (Huang and

NIH-PA Author Manuscript

NIH-PA Author Manuscript

NIH-PA Author Manuscript

Trussell, 2008) and then indirectly affect presynaptic [$Na^+$]. We therefore also recorded resting [$Na^+$] in the presence of TTX and found that CsCl still reduced the resting [$Na^+$] by 4.1 ± 1.0 mM ($P$ = 0.02, n = 4). Another HCN channel blocker ZD7288 (10-20 μM) showed a similar effect, reducing the resting [$Na^+$] by 4.0 ± 0.8 mM ($P$ = 0.04, n = 4; Fig. 2D).

## Blocking presynaptic HCN channels reduces quantal size

Given that the increase in [$Na^+$] facilitates vesicular glutamate uptake and increases mEPSC size, we predicted that blocking HCN channels, and thereby reducing intracellular [$Na^+$], would reduce the mEPSC amplitude. Using postsynaptic recordings, we measured mEPSCs while keeping the calyx intact (i.e., without presynaptic dialysis). In 10 of 14 recordings bath-application of 2 mM CsCl reversibly reduced the mEPSC amplitude by 14 ± 2% ($P$ = 0.002, n = 14; Fig. 3A-C & E) and shifted the cumulative frequency distribution to the left (Fig. 3D). Meanwhile, the mEPSC frequency slightly decreased from 2.7 ± 0.6 Hz to 2.4 ± 0.5 Hz ($P$ = 0.05). ZD7288 also showed an apparent non-specific effect by increasing mEPSC frequency, even in the presence of CsCl (from 2.1 ± 0.5 Hz to 3.5 ± 0.9 Hz; $P$ = 0.03, n = 5). However, we did not observe changes in mEPSC amplitude or frequency after adding CsCl in the continuous presence of ZD7288, suggesting the CsCl effect on the mEPSC is solely through blocking HCN channels. Because blocking postsynaptic HCN channels would not be expected to affect the mEPSC amplitude under our recording conditions (voltage clamp and extracellular $Cs^+$ perfusion), these experiments confirmed that the activity of presynaptic HCN channels control intracellular [$Na^+$], and thereby regulate quantal size.

## Modulation of HCN channels and quantal size

Studies in numerous preparations, including the calyx of Held (Cuttle et al., 2001), suggest that cAMP shifts the activation voltage of HCN conductance to more positive voltages, thereby enhancing the contribution of the current to the cell's resting state. We confirmed that indeed 8-Br-cAMP, a membrane-permeant cAMP analog, shifted the half-activation voltage by 13 mV (Fig. 4A). We also measured the [$Na^+$] change in the presence of TTX and found that 8-Br-cAMP (1 mM) increased presynaptic [$Na^+$] by 7.7 ± 2.3 mM ($P$ = 0.04, n = 4; Fig. 2E). To examine how 8-Br-cAMP affected mEPSC amplitude, recordings were made in the presence of selective inhibitors of protein kinase A (10 μM H-89 and/or 0.2 μM KT5720) to block possible postsynaptic effects of kinase activation. We found that bath-application of 8-Br-cAMP (0.5 mM) increased mEPSC amplitude by 19 ± 6 % ($P$ = 0.04, n = 4; Fig. 4B and C). To confirm that the increase of mEPSC amplitude by 8-Br-cAMP is indeed through activating HCN channels, we repeated the experiment in the presence of CsCl and found that 8-Br-cAMP no longer affected the mEPSC amplitude (4 ± 4%; $P$ = 0.24, n = 5; Supplemental Fig. S3, A-B). Forskolin, an adenylate cyclase activator, also shifted the half-activation voltage by 15 mV (Fig. 4D) and increased the mEPSC amplitude by 23 ± 5% ($P$ = 0.003, n = 6; Fig. 4E and F). Both 8-Br-cAMP and forskolin also increased the mEPSC frequency by 72 ± 16% ($P$ = 0.02) and 184 ± 38 % ($P$ = 0.003), respectively. It was of interest to determine whether the regulation of quantal size also applies to vesicles released by presynaptic action potentials, since these vesicles might have properties different from those generating mEPSCs. Thus, spike-evoked quanta were revealed by enhancing asynchronous release by substituting extracellular $Ca^{2+}$ by $Sr^{2+}$. Spikes triggered by an

NIH-PA Author Manuscript

NIH-PA Author Manuscript

NIH-PA Author Manuscript

extracellular electrode led to an obvious period of asynchronous releases (aEPSCs) following an initial fast EPSC current (Supplementary Fig. S3C). We measured the amplitudes of aEPSCs before and after application of 8-Br-cAMP and found that aEPSC amplitudes increased by 21± 5% ($P = 0.01$, n = 5). Thus, we conclude that alteration of intraterminal $Na^+$ concentration affects loading of vesicles regardless of how they are released.

## Discussion

Our results reveal a previously unknown mechanism by which a plasma membrane ion channel controls the strength of synaptic transmission by modulating vesicular content. A recent study showed that synaptic vesicles express a $K^+/H^+$ monovalent cation exchanger that stimulates vesicular glutamate transport (Goh et al., 2011). We found in this study that presynaptic $Na^+$ facilitates glutamate uptake and that a change in presynaptic $Na^+$ affects quantal size in the presence of constant $K^+$. Moreover, we estimated for the first time the resting concentration of $Na^+$ in a nerve terminal, and showed that changes in the activity of presynaptic HCN channels affected both intracellular $Na^+$ concentration and the quantal size.

The results indicate that presynaptic $Na^+$ is more potent than $K^+$ in facilitating glutamate uptake. In the presence of normal $K^+$ of 92 mM, presynaptic dialysis of 40 mM $Na^+$ increased the mEPSC amplitude by over 50% compared to that in $Na^+$-free solution. It should be noted that in these experiments the continuous activity of presynaptic ion channels, transporters and pumps that affect $Na^+$ levels in neurons may oppose $Na^+$ manipulation during whole-cell dialysis, and therefore the intracellular [$Na^+$] may be higher than 0 mM when dialyzed with $Na^+$-free solution and, conversely, lower than 40 mM when dialyzed with solution with 40 mM $Na^+$. If so, then quantal size may depend even more sharply on $Na^+$ than we observed.

There are three main types of ion channel in the calyx of Held that are active at resting membrane potentials: HCN, persistent $Na^+$ and KCNQ channels (Cuttle et al., 2001; Huang and Trussell, 2008, 2011). Because they are voltage dependent, activity of one may affect that of the others. Among these three channels, two are $Na^+$-permeable, including persistent $Na^+$ and HCN channels. Although the persistent $Na^+$ channel is active at the resting potential, we did not observe changes in quantal size when persistent $Na^+$ channels were blocked with 0.5 μM TTX (data not shown). However, we note that blocking this channel hyperpolarizes the membrane potential (Kim et al., 2007; Huang and Trussell, 2008) and thus further activates HCN channels. Thus, reduction of $Na^+$ by blocking $Na^+$ channels may be compensated by activation of HCN channels.

We found that presynaptic HCN channels control intracellular resting $Na^+$ concentration, such that blocking HCN reduces intracellular $Na^+$ concentration and reduces mEPSC amplitude while activation of HCN channels increases quantal size. Moreover, blocking HCN channels with CsCl reduced mEPSC frequency while enhancing HCN channel activation by 8-Br-cAMP or forskolin application increased mEPSC frequency. These effects may be partially due to a change in resting membrane potential following alteration

NIH-PA Author Manuscript

NIH-PA Author Manuscript

NIH-PA Author Manuscript

in HCN channel activity, given the membrane potential dependence of neurotransmitter release probability (Awatramani et al., 2005). The Epac pathway may also contribute to cAMP-dependent facilitation of neurotransmitter release probability (Kaneko and Takahashi, 2004). Another potential source of $Na^+$ to the calyx are the voltage gated $Na^+$ channels activated during action potentials, although it has been suggested that these channels are not prominent in the calyx (Leao et al. 2005). However, testing the effect of spike-derived $Na^+$ flux on mEPSC size would be challenging given that $Na^+$ levels after a spike train would likely fall faster than the time required for vesicle replenishment and reequilibration with transmitter after spike-triggered fusion (Fig 1). In this regard, HCN channels, which are activated near resting voltages, provide a more optimal mechanism for longer term changes in $Na^+$ levels in the terminal. Interestingly, the activation of HCN channels on glutamatergic terminals inhibited the frequency of mEPSCs in entorhinal cortical layer III neurons (Huang et al., 2011). This may be because the activation of HCN channels depolarizes the terminals and then reduces the availability of low-threshold, voltage-gated T-type $Ca^{2+}$ channels (Huang et al., 2011). However, in the calyx of Held, previous studies showed that the P/Q-type $Ca^{2+}$ channel is the dominant or only $Ca^{2+}$ channel type following hearing onset while T-type $Ca^{2+}$ channels are not expressed (Iwasaki and Takahashi, 1998; Wu et al., 1999).

The strength of excitatory synapses is determined by both presynaptic release probability and efficacy of postsynaptic receptors. It is generally accepted that the changes in frequency of mEPSCs reflects an alteration of presynaptic neurotransmitter release probability, and that the changes in mEPSC amplitude indicate postsynaptic alterations in neurotransmitter receptor interactions. Our results suggest caution in interpreting studies which use mEPSC amplitude to determine whether postsynaptic neurotransmitter receptor change during synaptic plasticity. During high-frequency spike activity, or during modulation that can alter the open probability of presynaptic channels, intracellular $Na^+$ may be altered and thereby result in alterations in quantal size that may be interpreted as a postsynaptic site of plasticity. More generally, our results suggest that neuromodulation affecting ion channels may control synaptic strength through the changes in the concentration of transmitter in synaptic vesicles.

## METHODS

### Slice Preparation

The handling and care of animals were according to procedures approved by the Institutional Animal Care and Use Committee of Oregon Health and Science University. Coronal brainstem slices containing the MNTB were prepared from P8-20 Wistar rats. Briefly, 180-210 μm sections were prepared in ice-cold, low-$Ca^{2+}$, low-$Na^+$ saline using a vibratome (VT1200S; Leica). Immediately after the slices were cut, they were incubated at 35°C for 20-60 min in normal ACSF and thereafter stored at room temperature. The saline for slicing contained (in mM) 230 sucrose, 25 glucose, 2.5 KCl, 3 $MgCl_2$, 0.1 $CaCl_2$, 1.25 $NaH_2PO_4$, 25 $NaHCO_3$, 0.4 ascorbic acid, 3 *myo*-inositol, and 2 Na-pyruvate, bubbled with 5% $CO_2$/95% $O_2$. The ACSF for incubation and recording contained (in mM) 125 NaCl, 25

NIH-PA Author Manuscript

NIH-PA Author Manuscript

NIH-PA Author Manuscript

glucose, 2.5 KCl, 1 $MgCl_2$, 2 $CaCl_2$, 1.25 $NaH_2PO_4$, 25 $NaHCO_3$, 0.4 ascorbic acid, 3 *myo*-inositol, and 2 Na-pyruvate, pH 7.4 bubbled with 5% $CO_2$/95% $O_2$.

## Whole-Cell Recordings

Slices were transferred to a recording chamber and were continually perfused with ACSF (2–3 ml/min) warmed to ~32 °C by an inline heater (Warner Instruments). Neurons were viewed using custom Dodt contrast optics and a water-immersion objective (Olympus) with a Zeiss Axioskop-2 microscope and an oil condenser (Nikon). Pipettes pulled from thick-walled borosilicate glass capillaries (WPI) and filled with recording solutions described below had open tip resistances of 3–5 MΩ and 2–3 MΩ for the pre- and postsynaptic recordings, respectively. Whole-cell voltage- and current-clamp recordings were made with a Multiclamp 700B amplifier (Molecular Devices). Calyceal terminals and postsynaptic MNTB neurons were identified by their appearances in contrast optics and/or Alexa 594 (10-20 μM) fluorescence.

For pair-recordings, presynaptic pipette solutions contained (in mM): 60 K-methanesulfonate, 20 KCl, 1 $MgCl_2$, 10 HEPES, 4 Mg-ATP, 0.3 $Tris_3$-GTP, 14 $Tris_2$-phosphocreatine, 1 glutamate, 0.2 EGTA, as well as (for 40 mM $Na^+$ solution) 40 Na-methanesulfonate, (for $Na^+$-free solution) 40 NMDG-methanesulfonate, or (for 10 mM $Na^+$ solution) 10 Na-methanesulfonate + 30 NMDG-methanesulfonate. All solutions were adjusted to pH 7.3 with KOH (290 mOsm) and the final $K^+$ for all solutions was 92 mM. Postsynaptic pipette solutions contained (in mM): 110 Cs-methanesulfonate, 5 CsCl, 1 $MgCl_2$, 4 Mg-ATP, 0.4 Tris-GTP, 14 $Tris_2$-phosphocreatine, 10 HEPES, 5 EGTA (290 mOsm, pH 7.3 with CsOH). In some experiments, the postsynaptic pipette contained (in mM): 110 K-gluconate, 15 KCl, 5 NaCl, 4 Mg-ATP, 0.3 $Tris_3$-GTP, 14 $Tris_2$-phosphocreatine, 10 HEPES, 0.2 EGTA (290 mOsm; pH 7.3 with KOH). Recording ACSF contained 5 μM (R)-CPP, 10 μM SR95531, 1 μM strychnine, and 0.5 μM TTX to block NMDA, GABA, glycine receptors, and voltage-gated $Na^+$ channel-mediated currents, respectively.

To record the presynaptic resting potential and presynaptic HCN current, pipette solution contained (in mM): 130 K-gluconate, 20 KCl, 0.2 EGTA, 10 HEPES, 4 Mg-ATP, 0.3 $Tris_3$-GTP, 3 $Na_2$-phosphocreatine, 2 $Tris_2$-phosphocreatine (290 mOsm; pH 7.3 with KOH). For recordings of HCN current at voltage-clamp mode, 0.5 μM TTX and 20 μM XE991 were added to block $Na^+$ and KCNQ channels, respectively. In some experiments, 200 μM $CdCl_2$, 2 mM 4-AP and 5 mM TEA-Cl were also added to ACSF substituting for NaCl with equal osmolarity to block the $Ca^{2+}$, and $K^+$ channels, respectively.

Resting potential was determined in current clamp at zero holding current. Liquid junction potentials were measured for all solutions, and reported voltages were adjusted appropriately. Series resistances (4-25 MΩ) were compensated by up to 70% (bandwidth 3 kHz). Signals were filtered at 4-10 kHz and sampled at 20-50 kHz.

NIH-PA Author Manuscript

NIH-PA Author Manuscript

NIH-PA Author Manuscript

### Two-photon $Na^+$-imaging

A two-photon imaging system (Prairie Technologies) was used as described previously (Bender et al., 2010). The laser was tuned to 810 nm, epi- and transfluorescence signals were captured through 40X, 0.8 NA or 60X, 1.0 NA objectives and a 1.4 NA oil immersion condenser (Olympus). Fluorescence was split into red and green channels using dichroic mirrors and band-pass filters (epi: 575 DCXR, HQ525/70, HQ607/45; trans: T560LPXR, ET510/80, ET620/60; Chroma). Green fluorescence (SBFI) was captured with H8224 photomultiplier tubes (PMTs, Hamamatsu). Red fluorescence (Alexa 594) was captured with R9110 PMTs (Hamamatsu). Data were collected in frame-scan or line-scan modes. Pipette solution contained (in mM): 110 K-gluconate, 15 KCl, 5 NaCl, 0.2 EGTA, 10 HEPES, 4 Mg-ATP, 0.3 $Tris_3$-GTP, 14 $Tris_2$-phosphocreatine (290 mOsm; pH 7.3 with KOH), while 1 mM SBFI and 20 μM Alexa 594 were added to the pipette solution. In some experiments, TTX (0.5 μM) was added into the ACSF to block voltage-gated $Na^+$ channels.

HCN channel-mediated $Na^+$ signals were evoked by voltage-steps during whole-cell recordings. To measure the resting $Na^+$ signals, pipettes were subsequently detached after whole-cell dialysis with SBFI and Alexa 594 dyes when the fluorescence intensities are stable, with or without TTX as indicated in the text. After waiting at least 15 min., the effects of HCN channel blockers on resting $Na^+$ signals were then measured. Standard calibration methods were used to measure the absolute $Na^+$ concentrations (Rose, 2012). The solutions for in situ calibration of SBFI fluorescence contained (in mM): 20 KCl, 25 glucose, 10 HEPES, 130 (K-gluconate + Na-gluconate), and adjusted to pH 7.4 with KOH. 3 μM gramicidin D, 10 μM monensin, and 50 μM ouabain were also added into the calibration solutions before experiments.

### Drugs

Drugs were obtained from Tocris (ZD7288, Forskolin, XE991, and H-89), Abcam (SR 95531, (R)-CPP, and TTX), Life Technologies (SBFI and Alexa 594), and all others from Sigma.

### Analysis

Data were analyzed using Clampfit (Molecular Devices), Igor (WaveMetrics) and Image J (NIH). Boltzmann functions were used to describe HCN activation: $G = G_{Max} / (1+\exp(-(V - V_{half}) / k ) )$, where G is conductance in nS, $G_{Max}$ is the maximal conductance, V is the holding potential in mV, $V_{half}$ is the voltage for half-maximal activation in mV, and k is the slope factor in mV. For $Na^+$ calibration, data were normalized and fitted by Michaelis-Menten equation: $(\Delta G/R) = (G/R)_{max} \times [Na^+]_i / ([Na^+]_i + K_{app})$, where G/R is the ratio of green fluorescence relative to red fluorescence; (ΔG/R) is the change in fluorescence ratio measured at a given $[Na^+]_i$ divided by that at 0 mM $[Na^+]_i$; $(G/R)_{max}$ is the maximal change in fluorescence ratio and $K_{app}$ is the apparent $K_d$ of SBFI for $Na^+$.

Data are expressed as mean ± S.E.M. Statistical significance was established using paired t-tests, except as noted.

NIH-PA Author Manuscript

NIH-PA Author Manuscript

NIH-PA Author Manuscript

## Supplementary Material

Refer to Web version on PubMed Central for supplementary material.

## Acknowledgments

We thank Drs. Craig Jahr, Hsin-Wei Lu, Zhengquan Tang and Daniel Yaeger for comments and Dr. Kevin Bender for technical advice. Financial supported was provided by US National Institutes of Health grants DC012063 (H.H.), DC004450, NS028901 (L.O.T.) and a Tartar fellowship (H.H.).

## References

Awatramani GB, Price GD, Trussell LO. Modulation of transmitter release by presynaptic resting potential and background calcium levels. Neuron. 2005; 48:109–121. [PubMed: 16202712]

Bender KJ, Ford CP, Trussell LO. Dopaminergic modulation of axon initial segment calcium channels regulates action potential initiation. Neuron. 2010; 68:500–511. [PubMed: 21040850]

Cuttle MF, Rusznak Z, Wong AY, Owens S, Forsythe ID. Modulation of a presynaptic hyperpolarization-activated cationic current (I(h)) at an excitatory synaptic terminal in the rat auditory brainstem. J Physiol. 2001; 534:733–744. [PubMed: 11483704]

Goh GY, Huang H, Ullman J, Borre L, Hnasko TS, Trussell LO, Edwards RH. Presynaptic regulation of quantal size: K+/H+ exchange stimulates vesicular glutamate transport. Nat Neurosci. 2011; 14:1285–1292. [PubMed: 21874016]

Hnasko TS, Edwards RH. Neurotransmitter corelease: mechanism and physiological role. Annu Rev Physiol. 2012; 74:225–243. [PubMed: 22054239]

Hori T, Takahashi T. Kinetics of synaptic vesicle refilling with neurotransmitter glutamate. Neuron. 2012; 76:511–517. [PubMed: 23141063]

Huang H, Trussell LO. Control of presynaptic function by a persistent Na(+) current. Neuron. 2008; 60:975–979. [PubMed: 19109905]

Huang H, Trussell LO. KCNQ5 channels control resting properties and release probability of a synapse. Nat Neurosci. 2011; 14:840–847. [PubMed: 21666672]

Huang Z, Lujan R, Kadurin I, Uebele VN, Renger JJ, Dolphin AC, Shah MM. Presynaptic HCN1 channels regulate Cav3.2 activity and neurotransmission at select cortical synapses. Nat Neurosci. 2011; 14:478–486. [PubMed: 21358644]

Ishikawa T, Sahara Y, Takahashi T. A single packet of transmitter does not saturate postsynaptic glutamate receptors. Neuron. 2002; 34:613–621. [PubMed: 12062044]

Iwasaki S, Takahashi T. Developmental changes in calcium channel types mediating synaptic transmission in rat auditory brainstem. J Physiol. 1998; 509:419–423. [PubMed: 9575291]

Kaneko M, Takahashi T. Presynaptic mechanism underlying cAMP-dependent synaptic potentiation. J Neurosci. 2004; 24:5202–5208. [PubMed: 15175390]

Kim JH, Sizov I, Dobretsov M, von Gersdorff H. Presynaptic Ca2+ buffers control the strength of a fast post-tetanic hyperpolarization mediated by the alpha3 Na(+)/K(+)-ATPase. Nat Neurosci. 2007; 10:196–205. [PubMed: 17220883]

Leão RM, Kushmerick C, Pinaud R, Renden R, Li GL, Taschenberger H, Spirou G, Levinson SR, von Gersdorff H. Presynaptic Na+ channels: locus, development, and recovery from inactivation at a high-fidelity synapse. J Neurosci. 2005; 25:3724–38. [PubMed: 15814803]

Maycox PR, Deckwerth T, Hell JW, Jahn R. Glutamate uptake by brain synaptic vesicles. Energy dependence of transport and functional reconstitution in proteoliposomes. J. Biol. Chem. 1988; 263:15423–15428. [PubMed: 2902091]

Rose CR. Two-photon sodium imaging in dendritic spines. Cold Spring Harb Protoc. 2012; 2012:1161–1165. [PubMed: 23118361]

Tabb JS, Kish PE, Van Dyke R, Ueda T. Glutamate transport into synaptic vesicles. J. Biol. Chem. 1992; 267:15412–15418. [PubMed: 1353494]

Wu LG, Westenbroek RE, Borst JG, Catterall WA, Sakmann B. Calcium channel types with distinct presynaptic localization couple differentially to transmitter release in single calyx-type synapses. J Neurosci. 1999; 19:726–736. [PubMed: 9880593]

NIH-PA Author Manuscript

NIH-PA Author Manuscript

NIH-PA Author Manuscript

NIH-PA Author Manuscript
NIH-PA Author Manuscript
NIH-PA Author Manuscript



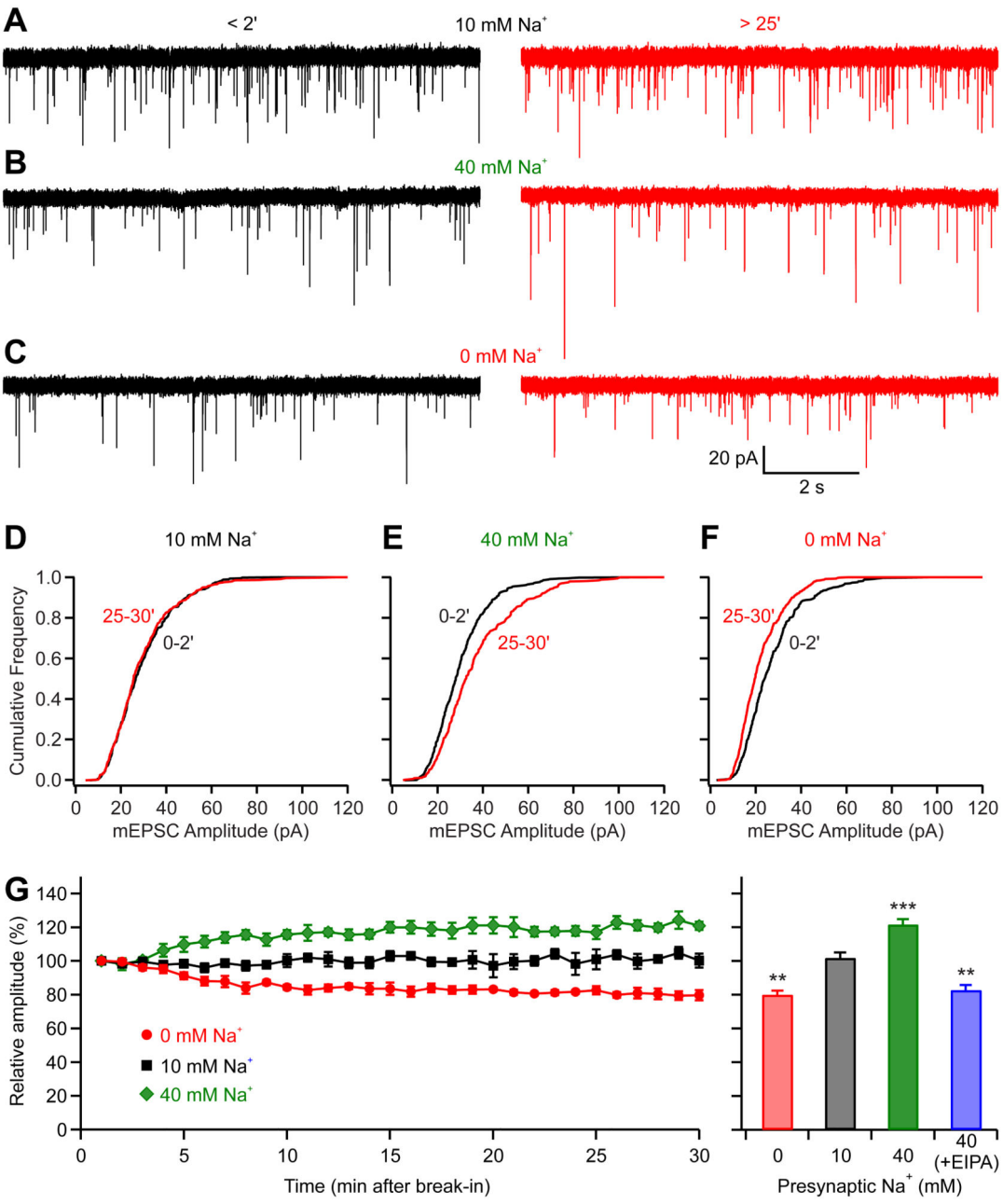


**Figure 1.**

Presynaptic intracellular $Na^+$ regulates mEPSC amplitude. (A-F) Pair-recordings were performed from both presynaptic calyceal terminal and postsynaptic MNTB principal neuron. The presynaptic pipettes contained either 10 mM (A, D), 40 mM (B, E), or 0 mM (C, F) $Na^+$, and the postsynaptic mEPSC were recorded. (A-C) Left panels were example recordings made < 2 min after presynaptic break-in while right panels were made > 25-min later. (D-F) Cumulative probability histograms of mEPSC amplitude early (black traces) and late (red traces) during dialysis are shown below the corresponding sweeps. (G) Time course of the average data from paired recordings for pipette solutions containing different $Na^+$ concentration. Each point represents 1 min of recording. Right panel shows that mEPSC

amplitudes at 25-30 min were relatively unchanged from those at 0-2 min when the pipettes were filled with 10 mM $Na^+$ solution, while the amplitudes were reduced with solution containing $Na^+$-free solution or increased significantly with 40 mM $Na^+$ solution. When EIPA was added to the 40 mM $Na^+$ solution, the mEPSC amplitudes were decreased rather than increased. **P < 0.01; ***P < 0.001; error bars, ± S.E.M.

NIH-PA Author Manuscript
NIH-PA Author Manuscript
NIH-PA Author Manuscript

NIH-PA Author Manuscript

NIH-PA Author Manuscript

NIH-PA Author Manuscript

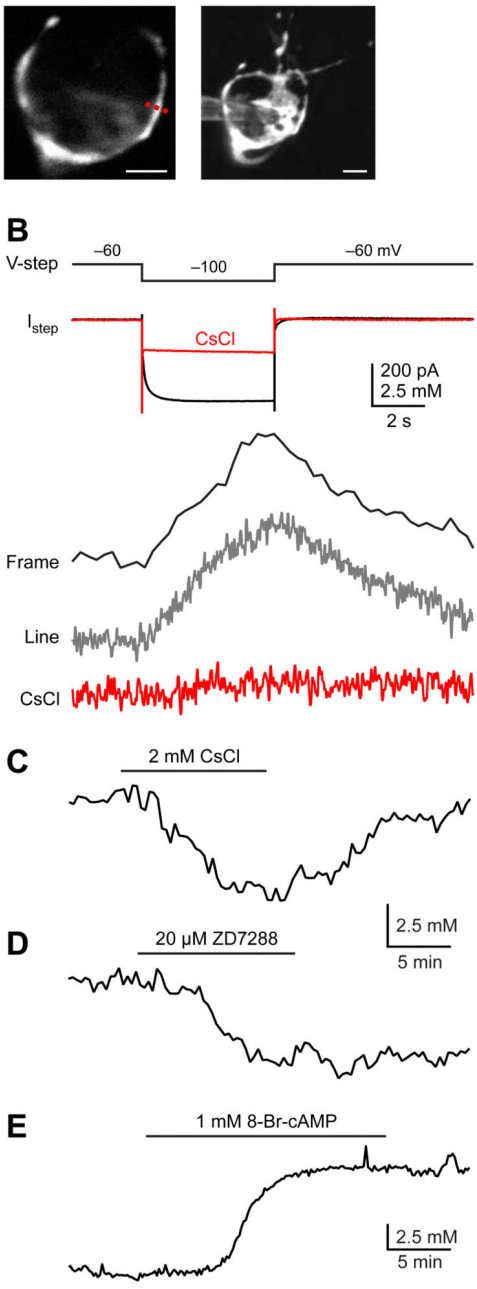


**Figure 2.**

Presynaptic HCN channels control resting $Na^+$ concentration. (A) Left panel: A single optical section of a calyx of Held using two-photon microscopy; Right panel: Maximum intensity montage of the calyx. Scale bars are 5 μm for both panels. (B) A voltage step to from −60 mV to −100 mV evoked an inward current. Meanwhile, a [$Na^+$] increase was visualized with SBFI under either frame-scan or line-scan modes. Both the inward current and Na transients were blocked by 2 mM CsCl. TTX was added to the ACSF to block voltage-gated $Na^+$ channels. (C-D) After dialysis with SBFI and Alexa 594, the recording pipettes were subsequently detached from calyces and the $Na^+$ signals were measured. At resting potentials, application of CsCl (C) or ZD7288 (D) reduced intracellular $Na^+$

concentrations. (E) 8-Br-cAMP increased intracellular resting $Na^+$ concentration. Note the difference in time scales in B and C-E.

NIH-PA Author Manuscript
NIH-PA Author Manuscript
NIH-PA Author Manuscript

NIH-PA Author Manuscript

NIH-PA Author Manuscript

NIH-PA Author Manuscript

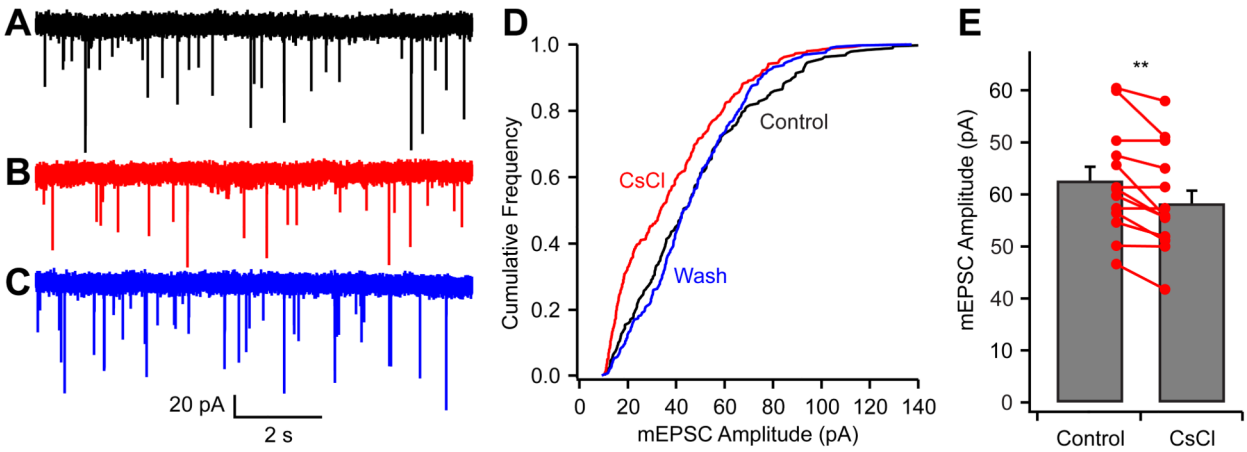


**Figure 3.**

Blocking HCN channels reduces mEPSC amplitude. (A-C) mEPSC recorded in control condition (A), in the presence of 2 mM CsCl (B), and after washout of CsCl (C). (D) Cumulative frequency distribution shows that CsCl reversibly reduced the mEPSC amplitudes. (E) Group data show CsCl effects on mEPSC amplitudes (n = 14). **P < 0.01; error bars, ± S.E.M.

NIH-PA Author Manuscript
NIH-PA Author Manuscript
NIH-PA Author Manuscript



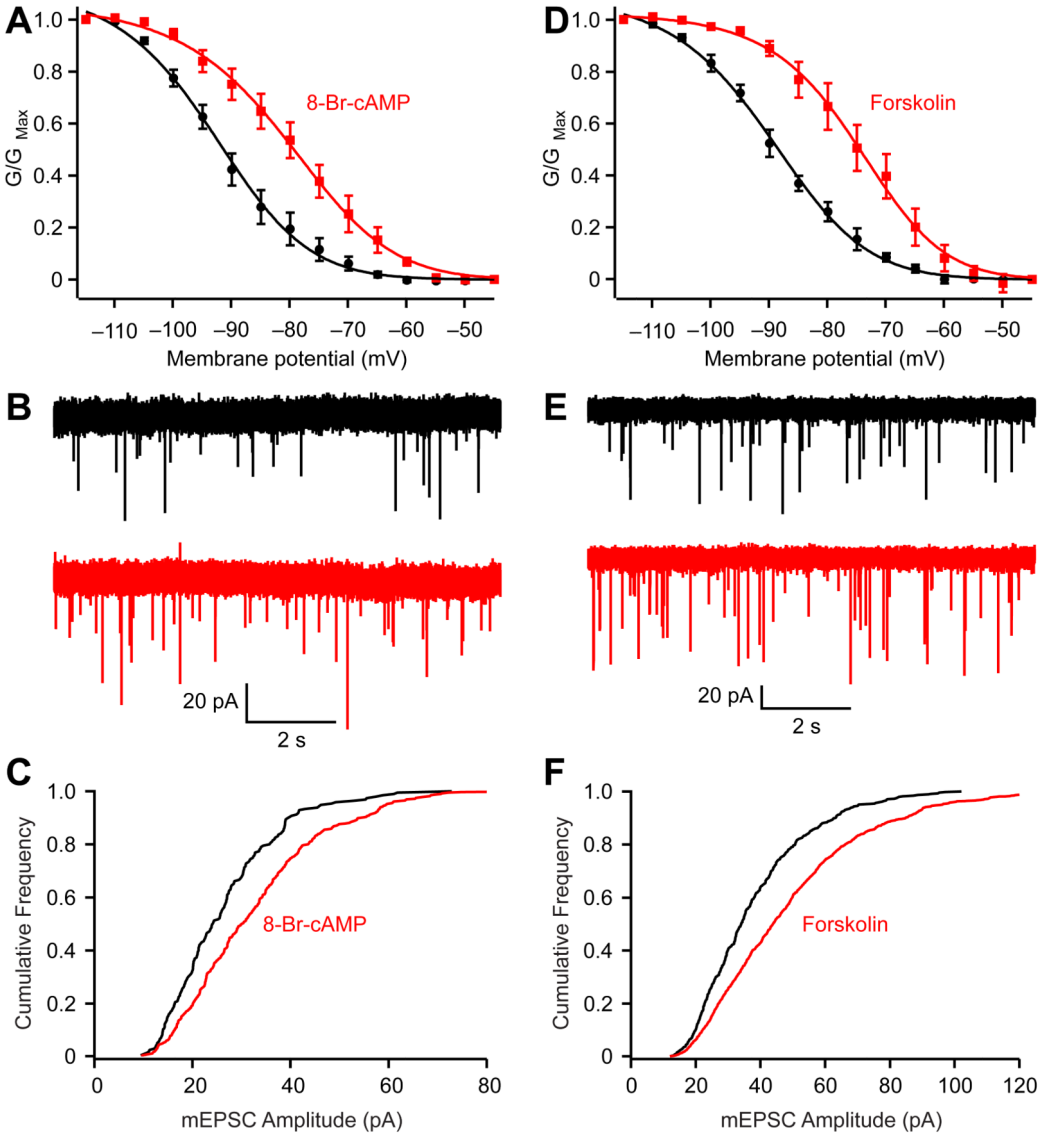


**Figure 4.**

Enhancing presynaptic HCN channel activation increases mEPSC amplitude. (A) 8-Br-cAMP (200-500 μM) right-shifted the activation curve of HCN channels (Control: $V_{half}$ = −93.3 ± 0.7 mV and slope = 11.1 ± 0.6 mV; 8-Br-cAMP: $V_{half}$ = −80.5 ± 0.5 and slope = 8.7 ± 0.4 mV. n = 5). (B-C) 8-Br-cAMP increased the mEPSC amplitudes (B) and right-shifted the cumulative probability histograms (C). (D-F) Forskolin (20 μM) also right-shifted the activation curve (Control: $V_{half}$ of = −90.0 ± 0.5 mV and slope = 11.5 ± 0.4 mV; Forskolin $V_{half}$ = −74.9 ± 0.5 mV and slope of 9.9 ± 0.5 mV. n = 5), increased the mEPSC amplitudes (E) and right-shifted the cumulative probability histogram (F). The voltage dependence of HCN activation was measured from HCN tail currents (TTX and XE991 were added to block $Na^+$ and KCNQ currents, respectively). Error bars, ± S.E.M.